Joint COS/CARP/MSTRC postgraduate student/postdoc workshop
18 September 2021

Venue: William M W Mong Engineering Building (ERB)
Lecture Theatre (8/F.)
The Chinese University of Hong Kong

Organized by: Centre of Optical Science (COS),
Centre for Advanced Research in Photonics (CARP), and
Materials Science and Technology Research Centre (MSTRC)

Programme

Optical Materials and Physics

Time	Speaker and Title
9:00 – 9:20 am	Yuwei Guo Perovskite light emitting diodes with high-radiance operational lifetime by phenylalkylammonium passivation
9:20 – 9:40 am	Shasha Li Generation and enhancement of strain-localized excitons in WS_2 monolayer by plasmonic metal nanocrystals
9:40 – 10:00 am	Yuan Li Anisotropic Dirac cone and slow edge states in a photonic Floquet lattice
10:00 – 10:20 am	Joshua Tin Yau Tse Why is the quality factor of bipartite SLR much higher than monopartite SLR?
10:20 – 10:40 am	Xiang Xi Determining the angular symmetry of optical force inside a material
10:40 – 11:00 am	Songshan Zeng Bio-inspired smart soft photonic materials
11:00 – 11:20 am	Ziyao Feng Phononic integrated circuitry with an etchless fabrication process
11:20 – 11:40 am	Fuhuan Shen Collective cavity-free polaritons in the photonic crystal based on bulk TMDCs materials
11:40 am – 12:00 pm	Jiapeng Zheng Motion control of plasmonic nanoparticles

Optical Devices and Instrumentation

Time	Speaker and Title
2:00 – 2:20 pm	Bingxu Chen Dual digital-micromirror-device pump-probe system
2:20 – 2:40 pm	Yanping He Single-frame label-free cell tomography for high throughput three-dimensional image cytometry applications
2:40 – 3:00 pm	Yujie Nie Transmission-matrix quantitative phase profilometry for accurate and fast surface profiling of thin films
3:00 – 3:20 pm	Yuanfei Zhang Magnification of slow light delay using four-wave mixing interferometer on a silicon chip
3:20 – 3:40 pm	Zunyue Zhang Integrated spectrometers on silicon photonics platform

3:40 – 4:00 pm	Yi Wang Two-dimensional layered $PtSe_2$ for high-speed optoelectronic devices
4:00 – 4:20 pm	Guodong Zhou Flexible ultrasensitive phototransistors for biomedical applications
4:20 – 4:40 pm	Dan Yi Multi-functional photonic processors using coherent network of micro-ring resonators
4:40 – 5:00 pm	Yingjie Shao Water-air optical wireless communication system based on the temporal and spatial properties of waves

Perovskite Light Emitting Diodes with High-radiance Operational Lifetime by Phenylalkylammonium Passivation

Yuwei Guo

Department of Electronic Engineering, The Chinese University of Hong Kong

Email: ywguo@link.cuhk.edu.hk

Abstract

Perovskite-based light emitting diodes (PeLEDs) display has a great potential in the display field. The past few years have seen a significant improvement in the efficiency of PeLEDs. However, the poor operation stability of the devices still hinders the commercialization of this technology in practical applications, exhibiting a rapid decay of external quantum efficiency (EQE) within minutes to hours during operation. To address this issue, we explore surface treatment of perovskite films with phenylalkylammonium iodide molecules of varying alkyl chain lengths. Combining experimental and theoretical analysis, we show that these molecules stabilize the perovskite through suppression of iodide ion migration. The stabilization effect is enhanced with increasing chain length due to the stronger binding of the molecules with the perovskite surface, as well as the increased steric hindrance to reconfiguration for accommodating ion migration. The passivation also reduces the surface defects, resulting in a high radiance and delayed roll-off of EQE. Using the optimized passivation molecule, phenylpropylammonium iodide, we achieve devices with an EQE of 17.5%, a radiance of 1282.8 W sr^{-1} m^{-2} and a T_{50} half-lifetime of 130 hrs under 100 mA cm^{-2}.

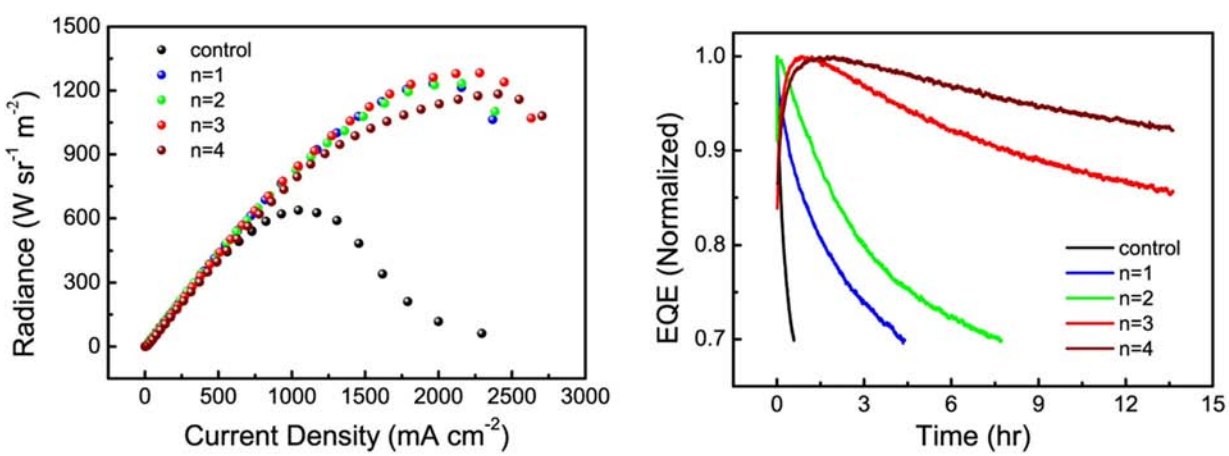

Generation and Enhancement of Strain-localized Excitons in WS_2 Monolayer by Plasmonic Metal Nanocrystals

Shasha Li,[†] Ka Kit Chui,[†] He Huang,[†] Shizheng Wen,[§] ChiYung Yam,[§] Lei Shao,[‡,§] and Jianfang Wang[†]

[†]*Department of Physics, The Chinese University of Hong Kong, Shatin, Hong Kong SAR, China*
[‡]*Shenzhen JL Computational Science and Applied Research Institute, Shenzhen 518131, China*
[§]*Beijing Computational Science Research Center, Beijing 100193, China*

Excitons in monolayer transition metal dichalcogenides (TMDs) can be modulated *via* strain with spatial and spectral control. [1, 2] The TMDs offer an ideal platform for constructing quantum emitters or single-photon sources, which are greatly desired for the on-chip quantum information processing applications. [3, 4] Strain localized excitons in TMDs have mainly been observed in cryogenic conditions because of their sub-wavelength emission area and low quantum yield. Integration of strained TMDs with plasmonic nanostructures or nanocavities provides a competitive approach for the detection of strain localized excitons at elevated temperatures. [5, 6] However, it is still challenging to construct quantum emitters in TMDs with large strain gradient and deterministically couple them to the plasmonic nanostructures. Herein we report on the generation and enhancement of strain-localized excitons in WS_2 monolayer at room temperature with the help of plasmonic metal nanocrystals that can be readily synthesized and support plasmon resonances overlapping with the exciton energy. The local strain is introduced by the deformation of a WS_2 monolayer placed on Au nanocrystals. Enhanced emission from strain-localized excitons in the WS_2–Au nanocrystal heterostructure is observed at room temperature with a large photoluminescence (PL) peak energy shift up to ~200 meV. The shape and size of the plasmonic nanocrystals largely affect the PL properties of the strain-localized excitons. Furthermore, the excitation and emission polarization of the strain-localized excitons are modulated using the anisotropic Au Nanorods. Our results provide a promising strategy for developing TMD-based integrated nanoscale light sources and photonic devices.

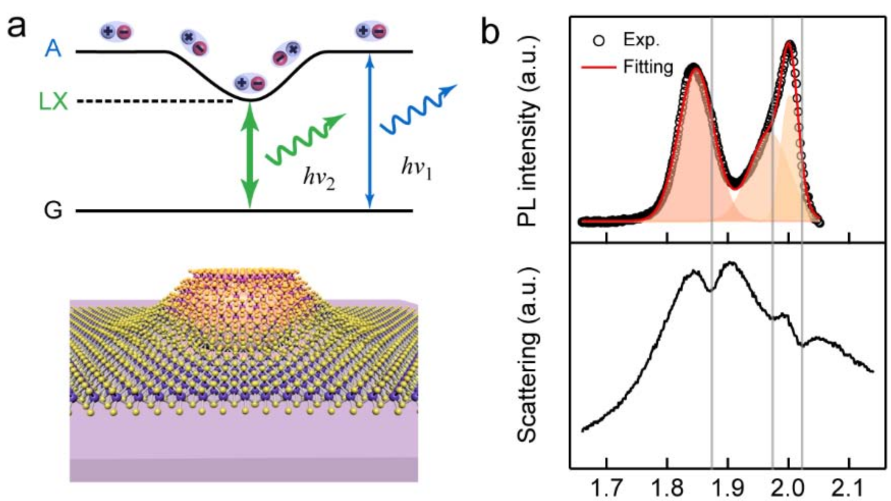

Figure 1. Generation and detection of strain-localized excitons in a WS_2 monolayer. (a) Schematic showing the working principle of the WS_2–Au nanocrystal heterostructure. (b) PL and dark-field scattering spectra of the heterostructure.

References

[1] Darlington, T. P.; Carmesin, C.; Florian, M.; Yanev, E.; Ajayi, O.; Ardelean, J; Rhodes, D. A.; Ghiotto, A.; Krayev, A.; Watanabe, K.; Taniguchi, T.; Kysar, J. W.; Pasupathy, A. N.; Hone, J. C.; Jahnke, F; Borys, N. J.; Schuck, P. J. Imaging strain-localized excitons in nanoscale bubbles of monolayer WSe_2 at room temperature. *Nat. Nanotechnol.* **2020**, *15*, 854−860.

[2] Li, H.; Contryman, A. W.; Qian, X. F.; Ardakani, S. M.; Gong, Y. J.; Wang, X. L.; Weisse, J. M.; Lee, C. H.; Zhao, J. H.; Ajayan, P. M. Li, J.; Manoharan, H. C.; Zheng, X. L. Optoelectronic crystal of artificial atoms in strain-textured molybdenum disulphide. *Nat. Commun.* **2015**, *6*, 7381.

[3] Branny, A.; Kumar, S.; Proux, R.; Gerardot, B. D. Deterministic strain-induced arrays of quantum emitters in a two-dimensional semiconductor. *Nat. Commun.* **2017**, *8*, 15053.

[4] Palacios-Berraquero, C.; Kara, D. M.; Montblanch, A. R.-P.; Barbone, M.; Latawiec, P.; Yoon, D.; Ott, A. K.; Loncar, M.; Ferrari, A. C.; Atatüre, M. Large-scale quantum-emitter arrays in atomically thin semiconductors. *Nat. Commun.* **2017**, *8*, 15093.

[5] Luo, Y.; Shepard, G. D.; Ardelean, J. V.; Rhodes, D. A.; Kim, B.; Barmak, K.; Hone, J. C.; Strauf, S. Deterministic coupling of site-controlled quantum emitters in monolayer WSe_2 to plasmonic nanocavities. *Nat. Nanotechnol.* **2018**, *13*, 1137–1142.

[6] So, J.-P.; Jeong, K.-Y.; Lee, J. M.; Kim, K.-H.; Lee, S.-J.; Huh, W.; Kim, H.-R.; Choi, J.-H.; Kim, J. M.; Kim, Y. S.; Lee, C.-H.; Nam, S. W.; Park, H.-G. Polarization control of deterministic single-photon emitters in monolayer WSe_2. *Nano Lett.* **2021**, *21*, 1546−1554.

Anisotropic Dirac cone and slow edge states in a photonic Floquet lattice

Yuan Li and Xiankai Sun*

Department of Electronic Engineering, The Chinese University of Hong Kong, Shatin, New Territories, Hong Kong

Corresponding author: xksun@cuhk.edu.hk

Abstract

Dirac cones with isotropic and linear dispersion, as in graphene, exhibit ultrahigh carrier mobility and offer an intriguing method to manipulate the behavior of particles. This concept has recently been extended to anisotropic Dirac cones with anisotropic dispersion in condensed matter, but their photonic counterparts are yet to be explored. Here, by introducing anisotropic coupling we propose a Floquet lattice with a realistic photonic scheme that supports anisotropic Dirac cones and abundant topological phases. Under the highly anisotropic circumstances, the presence of anomalous Floquet insulators is demonstrated, where topological slow edge states are found at a specific direction. The group velocity of the edge states can be tailored continuously by adjusting the anisotropy of the lattice. These slow edge states are robust against disorders and can be harnessed for developing intriguing applications such as anisotropic devices, topological delay lines, and optical nonlinear devices.

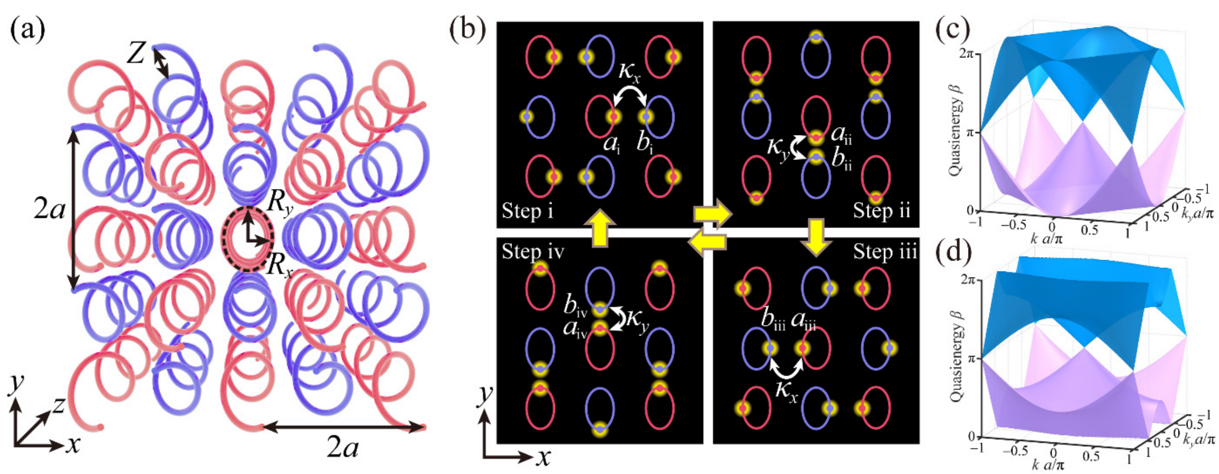

Fig. 1. Floquet system and band diagram. (a) Schematic illustration of a bipartite square lattice composed of evanescently coupled elliptic-helical waveguides. This bipartite square lattice is composed of A-type (red) and B-type (blue) sublattices, twisting counterclockwise along the propagation direction (z axis) with a relative shift. (b) Cross sections of the waveguide lattice showing the coupling between neighboring waveguides. In each step j (j = i, ii, iii, iv), the coupling between the neighboring waveguides occurs only along a specific direction. (c) Band structure of critical phase transition point ($\kappa_x = \kappa_y = \sqrt{2}/2$), which hosts an isotropic Dirac cone under the isotropic condition. (d) Band structure of critical phase transition point [$\arcsin(\kappa_x) = 0.15\pi$ and $\arcsin(\kappa_y) = 0.35\pi$], which hosts an anisotropic Dirac cone under the anisotropic condition.

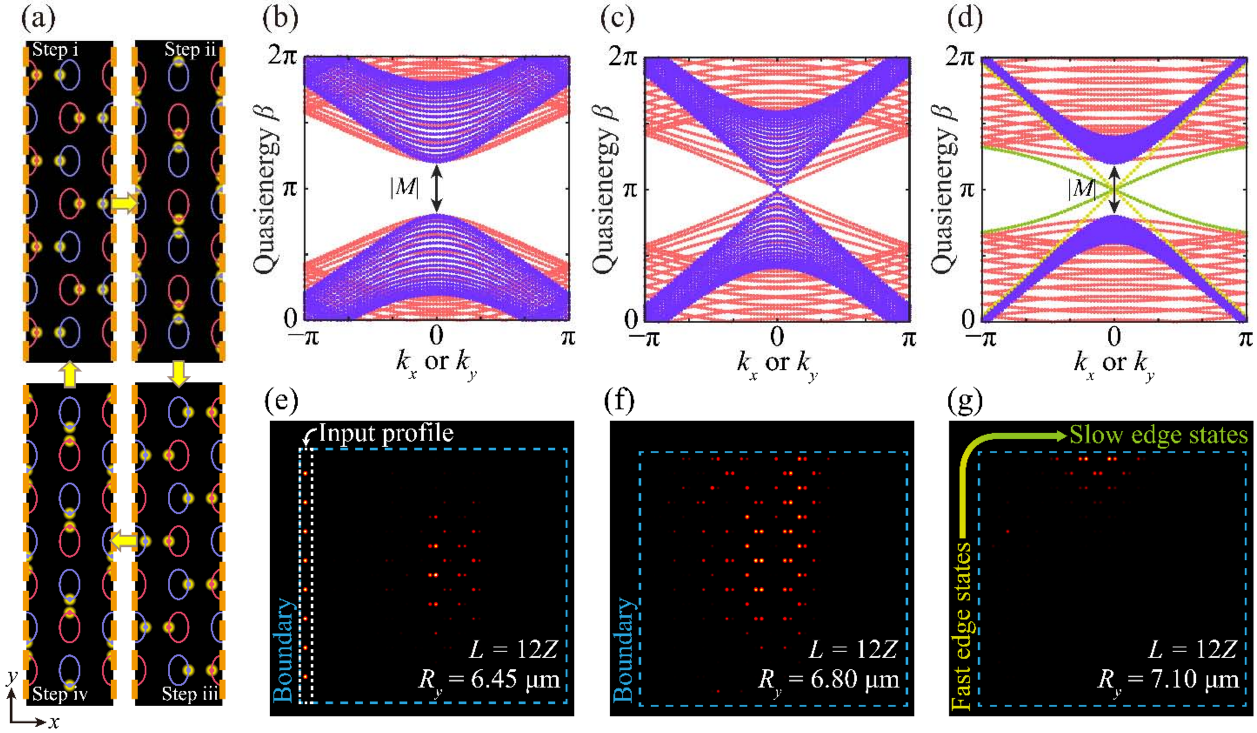

Fig. 2. Topological transition and edge-state band structures. (a) Schematic representation of a stripe structure composed of 7 unit cells, where the orange dashed lines represent the periodic boundary. (b)–(d) Edge-state band structures $\beta(\mathbf{k})$ along the x (red) and y (blue) directions with fixed $\arcsin(\kappa_x) = 0.15\pi$ ($R_x = 6.0$ μm) for trivial insulator with $\arcsin(\kappa_y) = 0.25\pi$ and $|M| = 0.4\pi$ ($R_y = 6.45$ μm) (b), for critical phase with $\arcsin(\kappa_y) = 0.35\pi$ and $|M| = 0$ ($R_y = 6.80$ μm) (c), and for anomalous Floquet insulator with $\arcsin(\kappa_y) = 0.45\pi$ and $|M| = 0.4\pi$ ($R_y = 7.10$ μm) (d). In (d) the yellow (green) dots plot the fast (slow) edge states with a larger (smaller) group velocity. (e)–(g) Numerically simulated output intensity profile $|\Psi(x, y, L)|^2$ for different topological phases. The blue dashed boxes represent the boundary of the lattice, and the white dashed box indicates the initial excitation distribution for (e)–(g). With the majority of edge states excited initially around $k_y = 0$, the output intensity profiles exhibit diverse propagation behaviors. Note that the fast edge states along the y direction convert adiabatically into the slow edge states along the x direction around the corner.

Why is the quality factor of bipartite SLR much higher than monopartite SLR?

Joshua Tin Yau Tse
Department of Physics, The Chinese University of Hong Kong

Keywords: surface lattice resonance (SLR), quality factor, temporal coupled-mode theory (CMT)

Abstract: Surface lattice resonance (SLR) is the hybridization of localized plasmon modes and propagating Rayleigh anomalies on metallic nanoparticle arrays. The nature of hybridization allows SLR to be engineered to possess high quality (Q) factor while maintaining a large mode volume. The high Q-factor of SLRs have been well documented, recent literature also shows SLR supported by nanoparticle dimer arrays have the potential to further enhance the Q-factor of SLRs than their monomer counterparts. However, how each factor in the design of a nanoparticle array contributes to enhancing the Q-factor is still largely unknown. In this presentation, I present the temporal coupled-mode theory (CMT) to model monopartite and bipartite SLRs. The scattering matrix of monopartite SLR is formulated and is cross-checked with time-domain FDTD simulations. The analytical Q-factor is also formulated based on CMT and was shown to depend quadratically on the spectral detuning. The CMT is then extended to bipartite SLRs where two identical nanoparticles are present in each unit cell and the coupling mechanisms between localized modes and Rayleigh anomalies are studied. The Q-factor was found to experience the same quadratic dependency on the detuning like the monopartite counterpart. However, the Q-factor can be further enhanced by directing the localized dark mode to couple with the Rayleigh anomalies and form SLRs with extraordinarily high Q-factor.

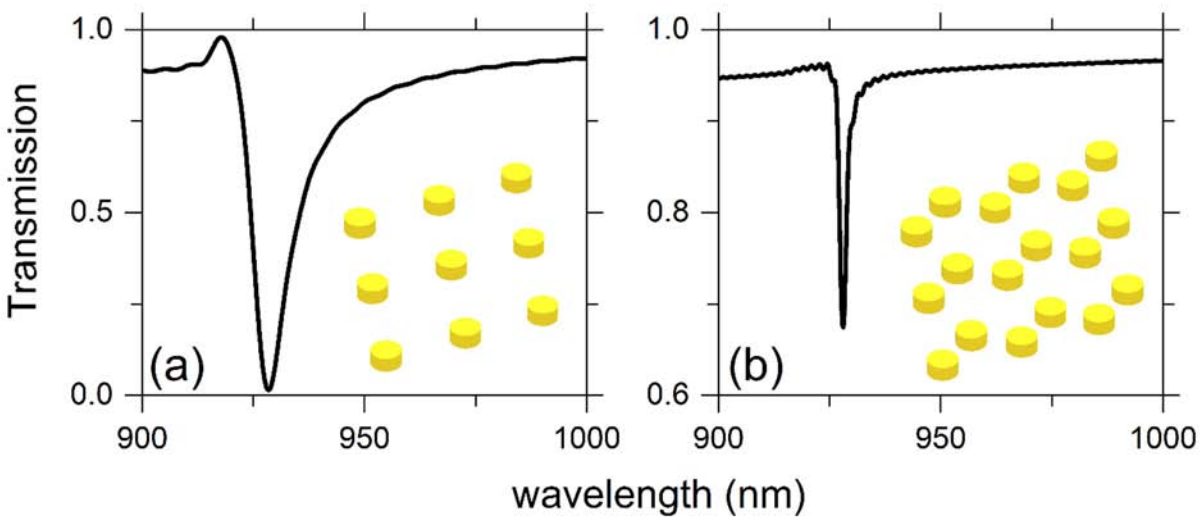

Figure 1. (a) Transmission spectrum of monopartite SLR. Inset: Illustration of monopartite nanoparticle array. (b) Transmission spectrum of bipartite SLR, showing significant improvement in quality factor from the monopartite counterpart. Inset: Illustration of bipartite nanoparticle array.

Determining the angular symmetry of optical force inside a material

Xiang Xi

Department of Electronic Engineering, The Chinese University of Hong Kong

Abstract: The textbook-accepted formulation of electromagnetic force was proposed by Lorentz in the 19th century, but its validity has been challenged due to incompatibility with the special relativity and momentum conservation. The Einstein–Laub formulation, which can reconcile those conflicts, was suggested as an alternative to the Lorentz formulation. However, intense debates on the two force formulations are still going on due to lack of experimental evidence. Most of the existing experiments fail to distinguish the two formulations because they predict the same total force on an object. Recently, it was theoretically discovered that the Lorentz and Einstein–Laub formulations produce different force distributions inside a dielectric medium. This feature can be harnessed in experiments to distinguish them. However, the predicted differences are microscopic and exist only inside a medium, which were thought to be too weak to be detected. Here, we report the first experimental investigation of angular symmetry of optical force inside a solid dielectric, aiming to distinguish the two formulations. The experiments surprisingly show that the optical force exerted by a Gaussian beam has components with the angular mode number of both 2 and 0, which cannot be explained solely by the Lorentz or the Einstein–Laub formulation. Instead, we found a modified Helmholtz theory by combining the Lorentz force with additional electrostrictive force could explain our experimental results. Our results represent a fundamental leap forward in determining the correct force formulation, and will update the working principles of many applications involving electromagnetic forces.

Figure:

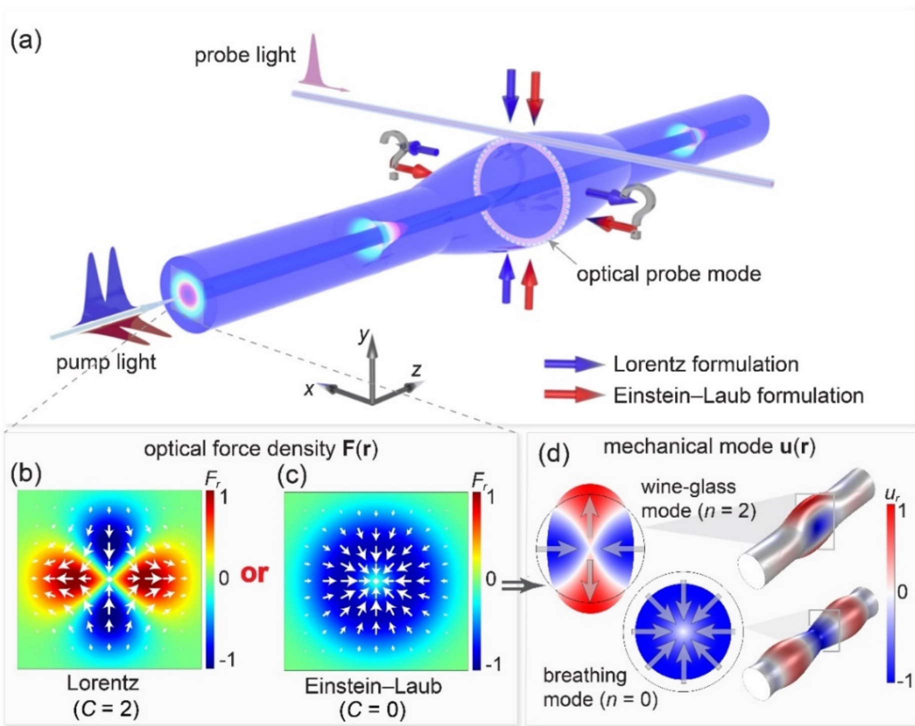

Bio-inspired Smart Soft Photonic Materials

Songshan Zeng and Zhaoli Gao
Department of Biomedical Engineering, The Chinese University of Hong Kong

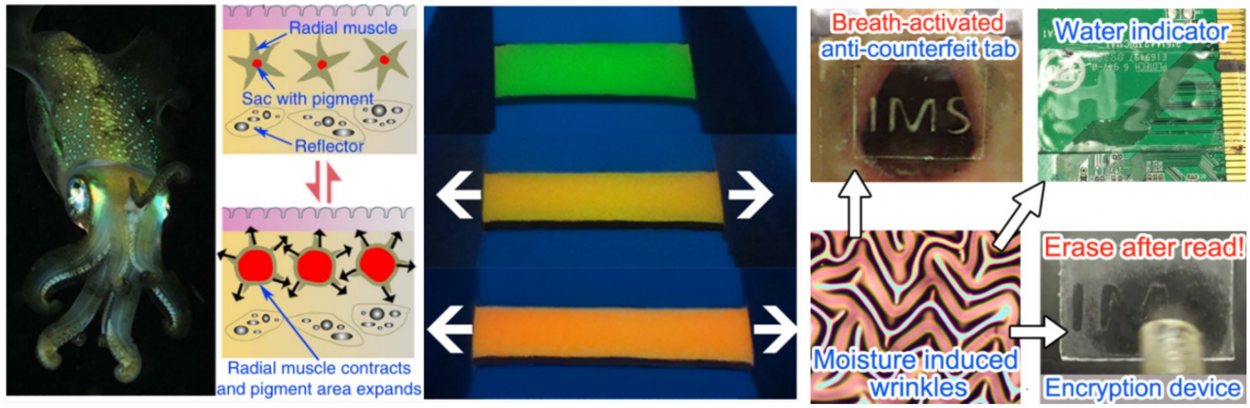

Smart soft photonic materials, capable of changing optical properties as exposed to external stimuli, have attracted tremendous research interest. Inspired by the intriguing stimuli responsive photonic properties in mother nature, a series of intriguing bilayer or multi-layer devices were achieved via multi-scale, multi-level structural design with various types of physical/chemical methods. These devices exhibit versatile multi-stimuli responsive characteristics which can dynamically change their optical properties (such as transparency, fluorescent intensity/coloration, reflectance and so on) as exposed to specific stimulus (such as heat, UV, moisture, electrical field and/or mechanical force). For instance, inspired by the display tactics in marine life, we developed a deformation-controlled surface-engineering approach via strain-dependent micro-cracks and folds to realize a broad range of mechanochromic devices with high sensitivity and reversibility. This techique can be further combined with a three-dimensional integration approach to achieve a set of multi-stimuli responsive chromic devices for stretchable interactive electronics, dynamic/static strain sensor and thermal radiation modulator. Further more, mimicing the wrinkling on the wet finger, we also realized three types of moisture-responsive wrinkled devices through a single film–substrate system. These unique responsive dynamics motivated the invention of a series of optical devices triggered by moisture. Other two related laser rewritable moisture responisve and multi-mechanical modes responsive wrinkle surfaces were also developed.

References

1. Zeng, S. et al. Bio-inspired Sensitive and Reversible Mechanochromisms via Strain-dependent Cracks and Folds. ***Nature Communications*** 2016, 7:11802.
2. Zeng, S. et al. Moisture-Responsive Wrinkling Surfaces with Tunable Dynamics. ***Advanced Materials*** 2017, 29, 1700828.
3. Zeng, S. et al. Dynamic Thermal Radiation Modulators via Mechanically Tunable Surface Emissivity. ***Materials Today*** 2021, 45, 44-53
4. Zeng, S. et al. Spontaneous Formation of Wrinkle-driven Tubular Structure as a Versatile Platform for Adaptive 3D Stretchable Electronics. ***Materials Horizons*** 2020, 7, 2368-2377.
5. Zeng, S. et al. Multi-stimuli responsive chromism with tailorable mechanochromic sensitivity for versatile interactive sensing under ambient conditions. ***Materials Horizons*** 2020, 7,164-172.
6. Zeng, S. et al. Smart laser-writable micropatterns with multi-scale photo/moisture

reconstructible structure. ***Advanced Functional Materials*** 2020, 31, 2009481
7. Zeng, S. et al. Tailoring multi-stimuli responsive micropatterns activated by various mechanical modes. ***Advanced Functional Materials*** 2021, 31, 2100612.
8. Wu, C.[#]; Zeng, S.[#]et al. Efficient Mechanoluminescent Elastomers for Dual-Responsive Anticounterfeiting Device and Stretching/Strain Sensor with Multimode Sensibility. ***Advanced Functional Materials*** 2018, 28, 1803168.

Phononic integrated circuitry with an etchless fabrication process

Ziyao Feng,[1,*] Yang Liu,[2] Lai Wang,[2] and Xiankai Sun[1]

[1]*Department of Electronic Engineering, The Chinese University of Hong Kong, Shatin, New Territories, Hong Kong*

[2]*Beijing National Research Center for Information Science and Technology (BNRist), Department of Electronic Engineering, Tsinghua University, Beijing 100084, China*

[*]*Email: 1155100869@link.cuhk.edu.hk*

Abstract: Recently, the concept of integrated photonic circuits to connect individual photonic devices has been expanded to the area in mechanics as integrated phononics. The guiding of the surface mechanical wave based on the piezoelectric material in an arbitrary route is crucial for the development and applications of integrated phononic circuits. To date, most mechanical waveguides work based on phononic crystals with relatively low frequency, large size, and complex fabrication process. Although stripe mechanical waveguides with simple design have been demonstrated, it is only applicable for limited piezoelectric materials bonded to specific substrates. Here, we theoretically proposed and experimentally demonstrated a new type of mechanical waveguides based on the pattern of a thin cladding layer to guide and bend the gigahertz mechanical wave. Guiding the surface mechanical wave also named as the Rayleigh mode through straight waveguides are experimentally demonstrated with the propagation loss around 7.50 dB/mm. Bending the mechanical wave through bent waveguides shows stronger confinement compared to other types of waveguides. We also found that the proposed waveguide could confine and guide Love mode which behaves as the bound states in the continuum. Multimode interference of mechanical wave to split mechanical wave in any ratio is further demonstrated. The proposed waveguide could also confine and guide the Love mode which behaves as the bound state in the continuum. Such waveguide could pave the way for the application of mechanical waves, such as information processing, sensing, and mechanical tweezers.

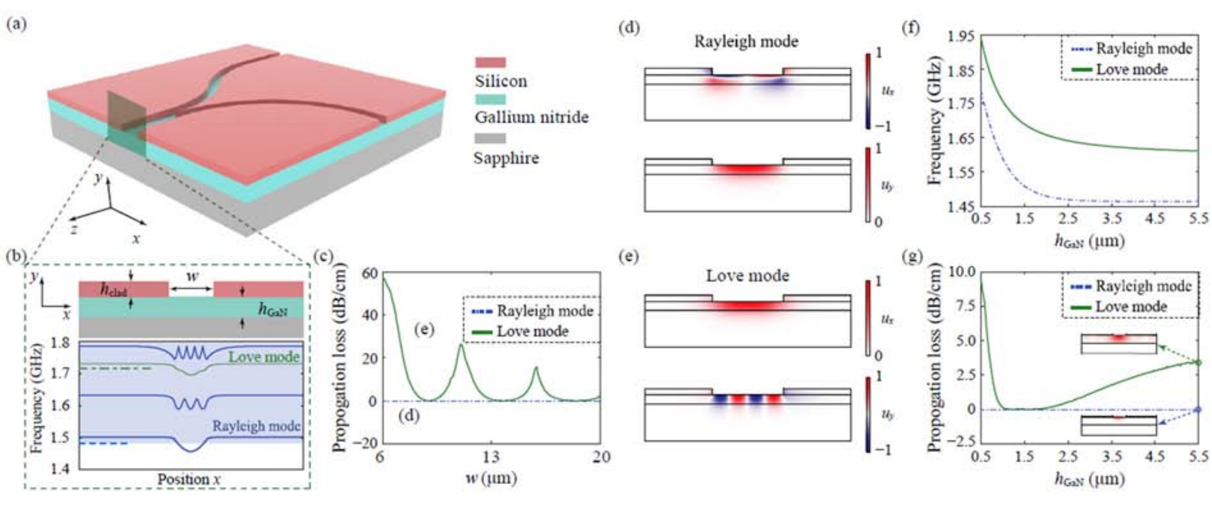

Collective Cavity-Free Polaritons in the Photonic Crystal Based on Bulk TMDCs Materials

Fuhuan Shen* and Jianbin Xu
Department of Electronic Engineering, The Chinese University of Hong Kong
Email: 1155116267@link.cuhk.edu.hk

Abstract
Room temperature exciton-polaritons, formed via the strong coupling of the TMDCs to the nanocavity, features abundant physical phenomena such as the optical nonlinearity and Bose Einstein condensation and are of great promise for the applications in the optoelectronic devices. Conventionally, extra cavity is required to strongly interact with the excitons within the TMDCs which is of great demand to integrate and manipulate in the subwavelength scale. In this work, based on the bottom up method, we demonstrate the room temperature collective polaritons in the monolithic photonic crystal(PC) made of the bulk MoS2(one of the TMDCs materials). To be specific, the Q factor up to 34.5 is achieved in the 1D PC and following spatial dispersion measurement reveals that the Rabi splitting reaches 300meV, exceeding dispassion rate of any components in the system. In addition, in the 2D PC the exciton-photon interaction is unambiguous observed with bulk excitons coupled with 2nd magnetic dipole(MD2) mode of the 2D PC . Our work paves the new way for achieving the room temperature polartions in more compact and integrated platform.

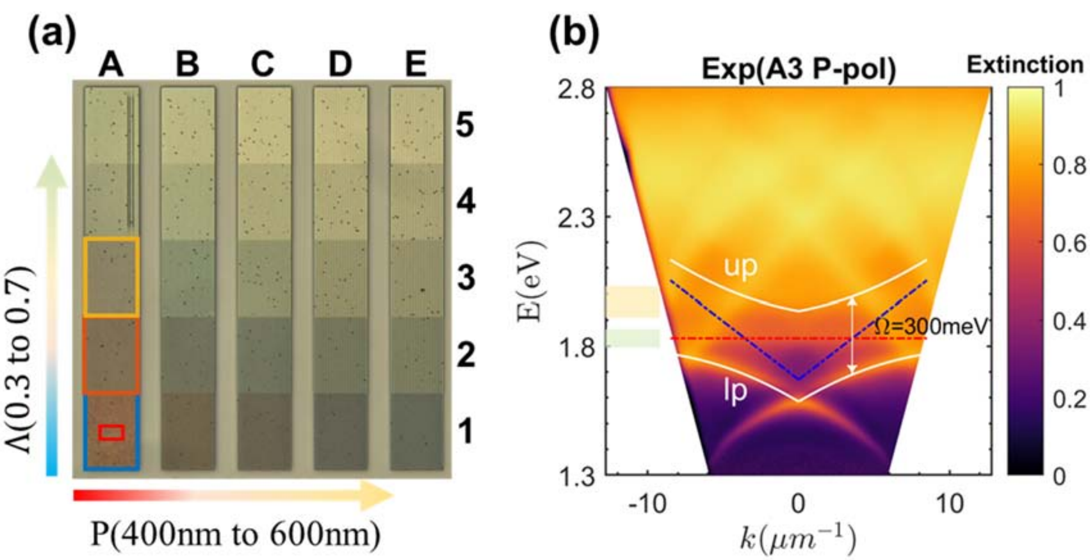

Fig. 1. (a) Optical picture of the 1D photonic crystal(PC). A-E represent different periods as shown in the bottom arrow and 1-5 represent different width/period ratios which is shown in the left arrow. (b) The spatial dispersion of the 1D PC where the blue dash-dot line is the dispersion of cavity, red dash-dot line represent the dispersion of A exciton and white lines represent the dispersions upper polartions(up) and lower polartions(lp).

Motion Control of Plasmonic Nanoparticles

Jiapeng Zheng, Lei Shao, and Jianfang Wang
Department of Physics, The Chinese University of Hong Kong

Chemically synthesized plasmonic nanoparticles (NPs) are regarded as the attractive building blocks for the construction of nanophotonic devices because of their ability in strongly confining electromagnetic energy to the nanoscale.[1,2] To assemble plasmonic NPs into functional devices, one of the essential steps is to control their behaviors. In this workshop, I will present the motion control of plasmonic NPs in the solution and at the solid–liquid interface. I will first describe my studies on the electrophoretic movement of plasmonic pigments for dynamic color display (Figure 1a). Plasmonic pigments with various colors have been prepared and functionalized. By applying a weak electric field, the complete assembly and disassembly of the plasmonic pigments from the display surface are realized, leading to a high-contrast and high-saturation color display.[3] The plasmonic pigments are integrated into microfluidic chips to construct digital electrophoretic display devices. I will then present a new type of catalytically powered and plasmon-enhanced nanomotors based on Au NPs moving on Si substrates (Figure 1b). HF and H_2O_2 are used as the chemical fuels to propel the Au nanomotors. The plasmon-enhanced nanomotors can move with a clear trace engraved on the silicon surface. Theoretical simulations show that the Au nanomotors with catalytic activities and an asymmetric coverage of the surfactants establish a chemical gradient. The Au nanomotors are propelled by an osmotic flow. Their movement can be significantly accelerated by the plasmon resonance of the Au nanomotors under visible light illumination. The plasmon-enhanced, self-traced metal nanomotors can be further applied in the fabrication of Si nanostructures.

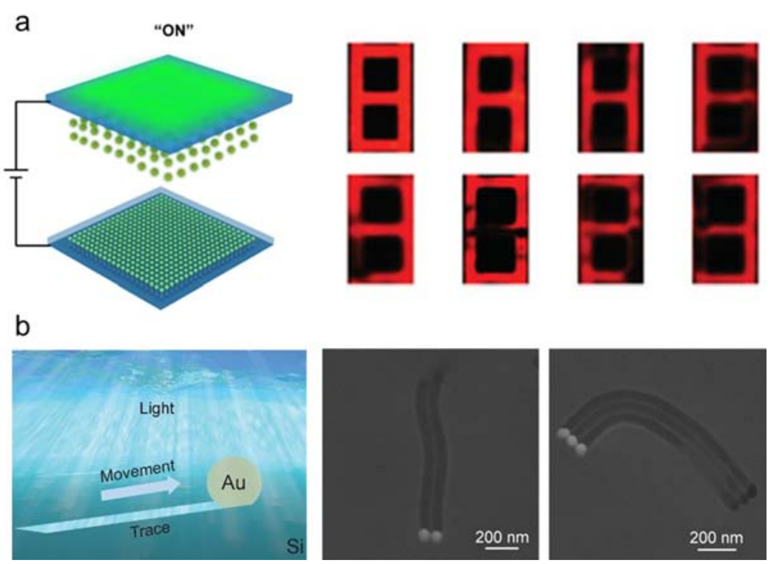

Figure 1. Motion control of plasmonic NPs. (a) Electrophoretic manipulation of plasmonic pigments for color display. Left: schematic illustration. Right: displayed patterns. (b) Plasmon-enhanced, self-traced nanomotors on the surface of silicon. Left: schematic illustration. Right: fabricated Si nanostructures.

[1] M. Ha, J. H. Kim, M. You, Q. Li, C. H. Fan, J.-M. Nam. Multicomponent plasmonic nanoparticles: from heterostructured nanoparticles to colloidal composite nanostructures. *Chem. Rev.* **2019**, *119*, 12208–12278.
[2] G. Baffoua, R. Quidant. Nanoplasmonics for chemistry. *Chem. Soc. Rev.* **2014**, *43*, 3898–3907.
[3] J. P. Zheng, T. H. Chow, S. S. Li, J. F. Wang, L. Shao. Electrophoretic plasmonic ink for dynamic color display. *Adv. Opt. Mater.* **2021**, *9*, 2100091.

Dual Digital-micromirror-device Pump-probe System

Bingxu Chen* and Shih-Chi Chen
Department of Mechanical & Automation Engineering, The Chinese University of Hong Kong
*Email: chenbx19@gmail.com

Keywords: Pump probe system, digital micromirror device (DMD)

Pump-probe microscopy is a specific implementation of a general approach, the use of nonlinear optical processes to improve molecular specificity, resolution, and penetration depth. As a pioneer of femto-chemistry, Nobel laureate Ahmed Hassan Zewail recorded the snapshots of chemical reactions with sub-angstrom resolution through an ultrafast femtosecond transient absorption (TA) technique in 1988. Pump-probe microscopy is an attractive imaging method with the following several reasons, comparing to other imaging techniques: nondestructive to cells, a label-free technique, three-dimensional spatial resolution due to its nonlinear optical technique, enhanced penetration depth, a lower level of tissue damage and so on.

A conventional pump-probe microscope uses galvanometers as scanning devices. However, the imaging speed cannot be increased significantly, due to the acquisition frequency and the mechanical scanners have its upper limit. To solve these mentioned problems, a digital micromirror device (DMD)-based pump probe microscope is proposed.

A DMD chip is the core component in a projector, which can be further used as a scanning element to replace the scanning galvanometer. In 2020, our group have invented a dual DMD pump-probe microscope, as shown in Fig.1(a). This design not only takes into account that DMD is sensitive to wavelength as a diffraction element, but also frees the scanning mode of two beams of light so that each beam can scan independently, which is totally different from the traditional system. Fig.1(b) shows the transient absorption images of Si-SiO_2 materials with different time delays.

Besides, this system can measure transient absorption properties of different kinds of materials, including diffusion rate of carriers at different time delays, reaction of materials to polarized light and relaxation time of materials to the pump. Fig.2 shows a typical example of transient absorption analysis of a kind of 2D material.

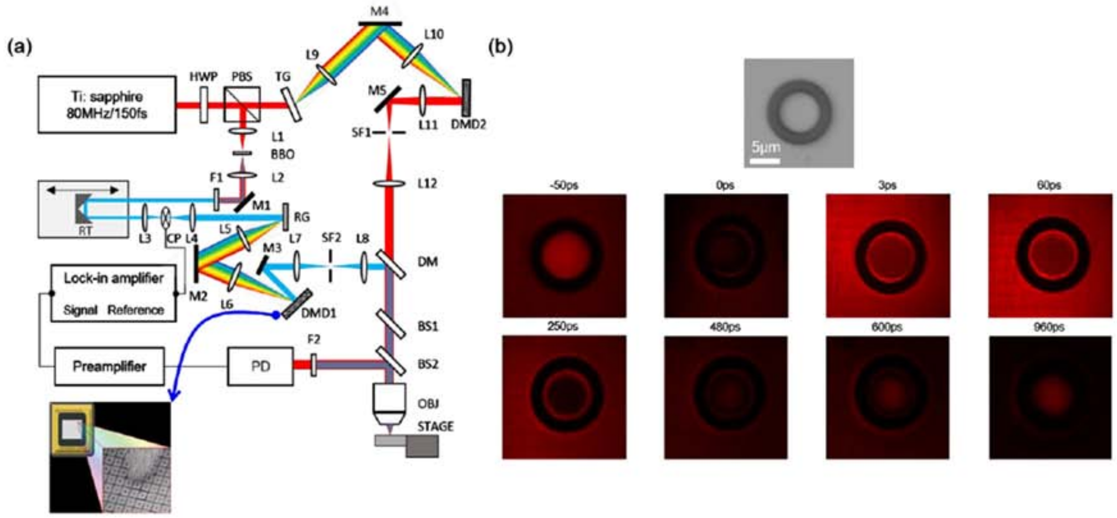

Figure 1. (a) Optical configuration of the dual-DMD pump-probe microscope system. (b) Transient absorption images of circle pattern of silicon on the silicon dioxide substrate. Scale bar: 5μm.

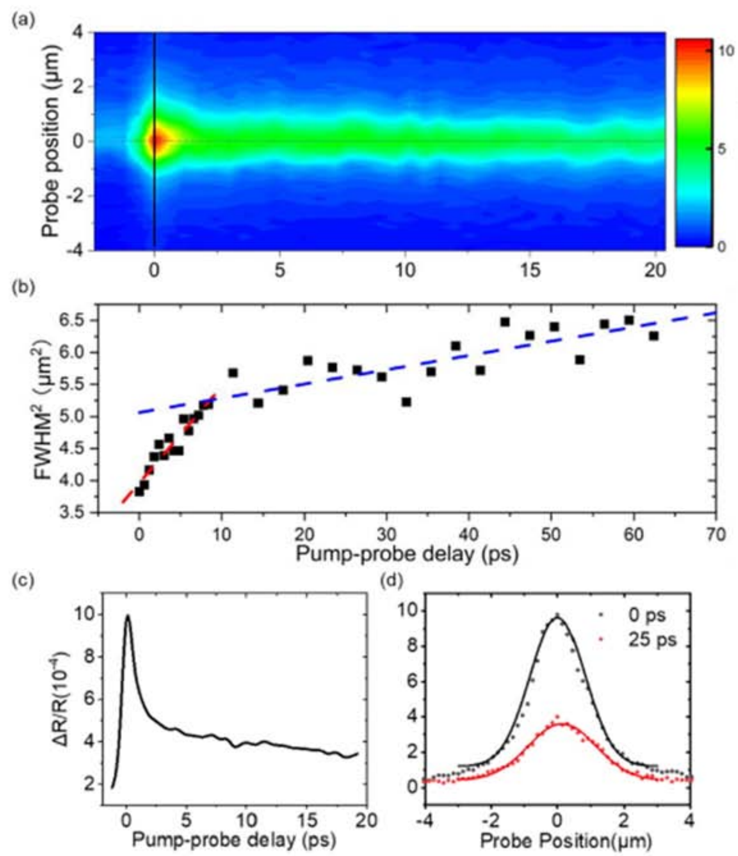

Figure 2. An example of transient absorption analysis of a kind of 2D material. (a) Spatiotemporal dynamics of the transient reflection signal ΔR/R. (b) Squared-width evolution of the ΔR/R profile, extracted by Gaussian fitting to the spatial profile at each pump-probe delay. (c) is the dotted line in (a). Transient reflectivity dynamics for collinear pump and probe pulses, exhibiting two distinct exponential decay contributions. (d) is the solid line in (a). Spatial profiles (dots) and Gaussian fits (curves) for two selected pump-probe delays.

Single-frame Label-free Cell Tomography for High Throughput Three-dimensional Image Cytometry Applications

Yanping He* and Renjie Zhou

Department of Biomedical Engineering, The Chinese University of Hong Kong, Shatin, New Territories, Hong Kong, China
**Corresponding author e-mail address: heyanping@link.cuhk.edu.hk*

250 words abstract

Image cytometry techniques have many potential applications in biomedical studies, such as stem cell classification, blood testing, etc. However, current image cytometry methods either provide limited morphological information or the throughput is limited. In recent years, optical diffraction tomography (ODT) has demonstrated a great potential for label-free live cell imaging by mapping their subcellular structures and quantifying their chemical compositions. Here we propose a new high throughput label-free 3D image cytometry method, called single-frame label-free cell tomography (SILACT), which is based on a recently proposed angle-multiplexed ODT method and a trained deep neural network (DNN) model for reconstructing 3D refractive index (RI) maps of cells. In SILACT, the 3D structure of a cell is reconstructed with only one single raw interferogram. By implementing a high-speed camera, we can capture the interferograms at over 10,000 frames per second, namely achieving the acquisition of over 10,000 tomograms per second without suffering from motion artifacts. By flowing the cells in a microfluidic chip and minimizing the camera exposure time, we have realized imaged of 20,000 cells per second. We envision that this new 3D image cytometry method will greatly improve the accuracy and efficiency over current cell analysis methods, therefore potentially offering new tools for research investigations in regenerative medicine, hematology, clinical studies, etc.

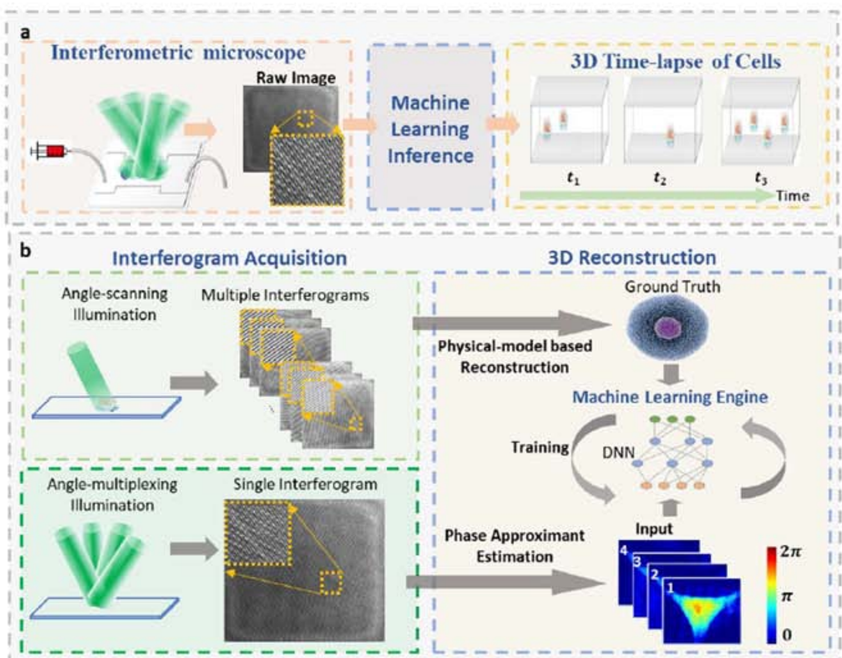

Figure 1. Illustration of the single-frame label-free cell tomography method. (a) The pipeline of 3D RI time-lapse video reconstruction with machine learning inference. (b) The training process of the machine learning engine. The upper part demonstrates the preparation of ground truth RI maps: the RI maps are produced by the physical-based reconstruction algorithm (i.e., Learning-based reconstruction model using the Beam Propagation Method) from all 49 interferograms captured under the angle-scanning illumination scheme. The lower part of (b) shows the input to the training process using the four crude phase maps estimated from the single interferogram measured under the angle-multiplexing illumination scheme.

Transmission-matrix Quantitative Phase Profilometry for Accurate and Fast Surface Profiling of Thin Films

Yujie Nie* and Renjie Zhou

Department of Biomedical Engineering, The Chinese University of Hong Kong,

Shatin, New Territories, Hong Kong, China

**Corresponding author e-mail address: nieyujie@link.cuhk.edu.hk*

250 words abstract:

Characterizing the surface profile of thin film structures is significant as these structures have potential uses in electronic devices and their morphology may affect the device functions. Current methods for profiling thin film structures include contact surface contourgraph, atomic force microscopy (AFM), scanning electron microscopy (SEM), and reflection interferometry. Contact surface contourgraph and AFM can obtain the topography of thin films, but they have a low imaging throughput and require direct contact with the sample through a special probe. Laser interferometry can measure the height map of thin samples without direct contact, and it can also achieve real-time imaging. To measure the surface profile of thin film samples with high precision and high speed, we propose a new imaging-based profilometer based on a common-path interferometry based quantitative phase microscope and a transmission-matrix model for thickness interpolation, which we call Transmission-matrix Quantitative Phase Profilometer (TM-QPP). In TM-QPM, a high well capacity camera is implemented to significantly reduce the shot noise contribution to the overall phase noise. The use of a common-path interferometry design has further allowed us to achieve a high temporal stability, thus resulting in a temporal phase sensitivity of better than 10 picometers, as characterized by the optical pathlength difference. As multiple interference in a thin film may affect the heigh interpolation accuracy, we developed the transmission-matrix based model to precisely determine the thickness from phase measurements. We verified the surface profiling capability of our system on MoS_2 thin films and our results match with AFM and Raman spectroscopy measurements, while our measurement time is within a few milliseconds. We envision this new surface profiling method will have many potential applications in material metrology and bioimaging.

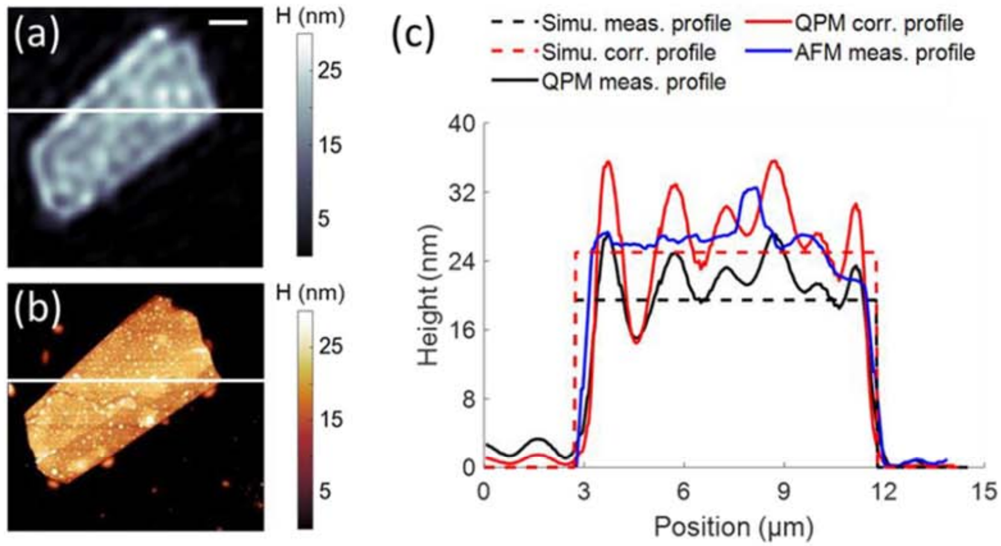

Figure 1. (a) and (b) AFM image and quantitative phase image of a MoS_2 flake, respectively. Scale bar: 2 μm. (c) A comparison of simulated surface profiles, measured surface profiles, and corrected surface profile along the white lines, as indicated in (a) and (b).

Magnification of Slow Light Delay Using Four-Wave Mixing Interferometer on a Silicon Chip

Yuanfei Zhang, Honghui Zhang, and Chester Shu
Center for Advanced Research in Photonics, Department of Electronic Engineering, The Chinese University of Hong Kong, Shatin, N.T., Hong Kong
Author e-mail address: yfzhang@link.cuhk.edu.hk

Abstract: In this work, we propose and demonstrate a phase-amplification scheme to magnify the broadband Brillouin-induced phase change, hence the slow light optical delay. Nonlinear interferometric processing is realized at the idler wavelength between a signal pulse with a fixed delay and a reference pulse through four-wave mixing on a silicon waveguide. The amplification and tunability of the optical delay are demonstrated. The delay of the synthesized pulse centered at the idler wavelength can be rapidly tuned by controlling the power of a non-delayed reference pulse. Using a silicon-based four-wave mixing interferometer, we apply the phase-amplification scheme to magnify the optical delay induced by stimulated Brillouin scattering (SBS) slow light. The initial SBS slow light delay of 300 ps introduced by a spectrally broadened Brillouin pump has been successfully varied from -160 to +1140 ps.

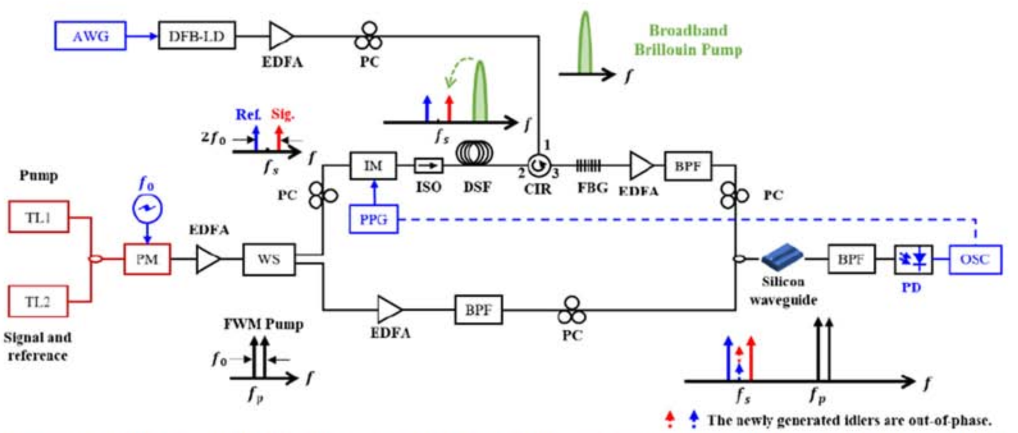

Fig. 1. Experimental setup for the magnification of slow light delay using four-wave mixing interferometer on a silicon chip. TL: tunable laser; PM: phase modulator; WS: WaveShaper; PC: polarization controller; IM: intensity modulator; AWG: arbitrary waveform generator; DFB-LD: distribute feedback Bragg laser diode; DSF: dispersion-shifted fiber; CIR: circulator; FBG: fiber Bragg grating; BPF: bandpass filter; EDFA: erbium-doped fiber amplifier; PD: photodetector; OSC: oscilloscope.

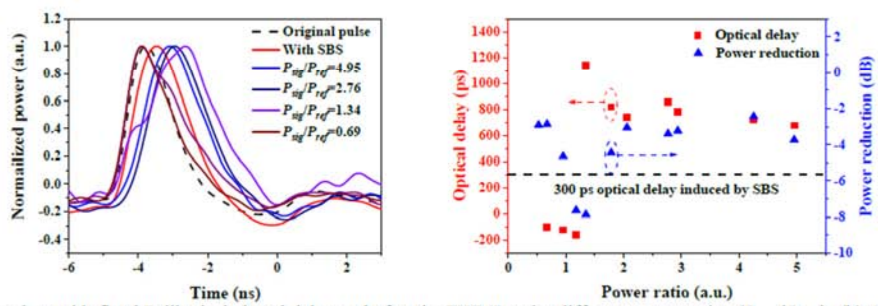

Fig. 2. (a) Output pulses with fixed Brillouin-induced delay and after the FWMI under different power ratios (P_{sig}/P_{ref}). (b) Amplified optical delay and power reduction of the optical pulses after under different power ratios.

Integrated Spectrometers on Silicon Photonics Platform

Zunyue Zhang
Department of Electronic Engineering, The Chinese University of Hong Kong
Email: zyzhang@link.cuhk.edu.hk

Abstract: Spectrally resolved interferometry is used in biosensing and bioimaging and has the advantages of high sensitivity and label free sensing. It has application in spectral domain optical coherence tomography (SD-OCT), which requires spectrometers to have both wide optical bandwidth and high spectral resolution. Silicon photonics offer the opportunity for the implementation of integrated optical spectrometers on the high index contrast silicon photonics platform. However, conventional spectrometers that rely on dispersive devices are hard to obtain high spectral resolution due to the long optical path lengths needed. My research work focuses on the implementation of advanced integrated spectrometers on silicon photonic platform towards the application in bioimaging and biosensing systems. Here I present two of our recent work on scanning spectrometer with both wide optical bandwidth and high spectral resolution, and the compact speckle spectrometer with ultrahigh spectral resolution. The integrated scanning spectrometer is composed of the high-resolution microring resonator (MRR) and wideband arrayed waveguide grating (AWG). The MRR is designed to have free spectral range equal the channels spacing of the AWG and with resonance wavelength tunable within the pass band of the AWG channel by using integrated micro-heater. A total of 350 wavelength channels that give 70 nm optical bandwidth and 0.2 nm channel spacing is demonstrated. The speckle spectrometer designed by using a linear coherent network is demonstrated to have 20 pm spectral resolution and enabled by compressive sensing algorithm, a 12-nm working window was obtained within the 520 µm × 220 µm device footprint.

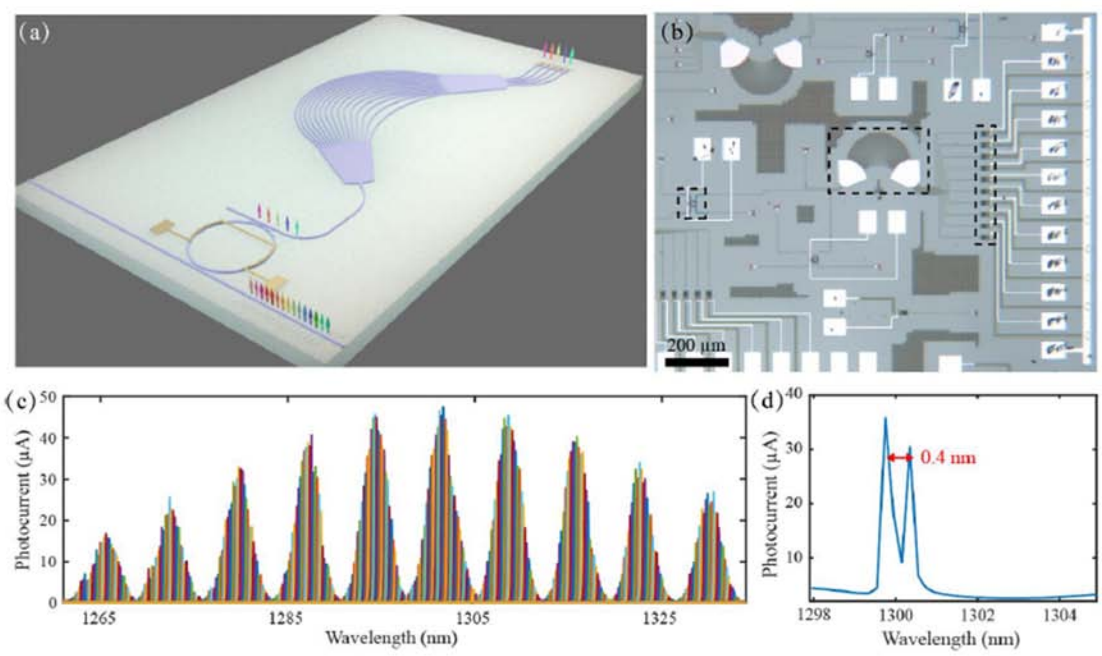

Fig. 1 (a) Schematic of the integrated scanning spectrometer. (b) Microscope image of the integrated scanning spectrometer. (c) Experimental transmission spectrum of all the 350 wavelength channels that cover 70 nm wavelength range. (d) Measurement result of two spectral lines with 0.4 nm spacing by using the integrated scanning spectrometer.

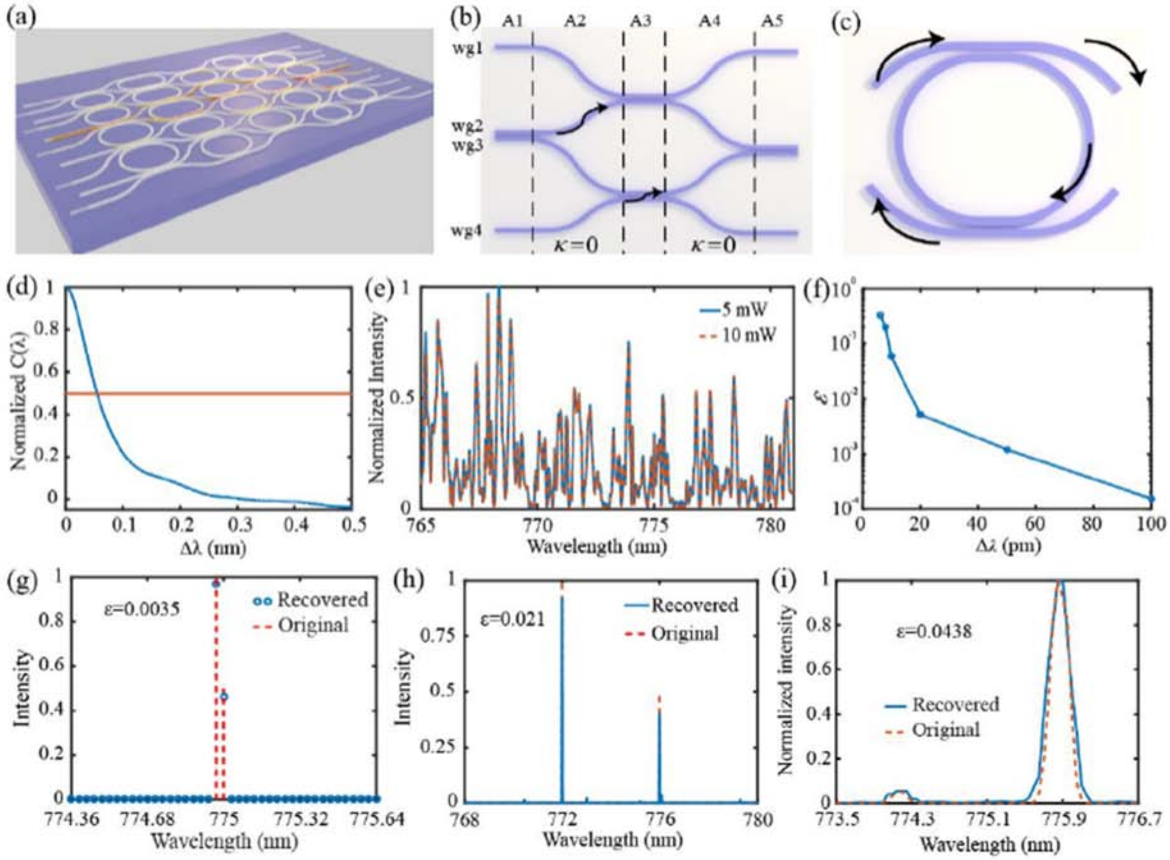

Fig. 2 (a) Schematic of the integrated speckle spectrometer. (b) Schematic of one building block of the mutually coupled MZIs, where κ is the coupling coefficient. (c) Schematic of one building block of the linear coherent network with MRR added into the mutually coupled MZI. (d) Calculated spectral correlation function of the 64-channel speckle spectrometer. (e) Normalized transmission spectra of No. 32 physical channel with input light power of 5 mW and 10 mW. (f) Relative errors of the recovered spectra with the increase of wavelength spacing between the two spectral lines. (g) Reconstructed spectral lines with spectral spacing of 20 pm. (h) Reconstructed sparse spectra with 2 spectral lines in a 12-nm operating bandwidth. (i) Reconstructed result of the transmission spectrum of one channel of arrayed waveguide grating.

Two-dimensional layered $PtSe_2$ for high-speed optoelectronic devices

Yi Wang and Hon Ki Tsang*

Department of Electronic Engineering, The Chinese University of Hong Kong, Shatin, Hong Kong SAR, P.R. China

**Email: hktsang@ee.cuhk.edu.hk*

Hybrid integration of two-dimensional (2D) materials on photonic integrated circuits (PICs) open a new avenue for integrated photonics because they offer additional functionality beyond those available with the native PIC platform, typically silicon nitride or silicon. For example, the unique properties of 2D materials like layer-tunable bandgap, high optical nonlinearity, direct band light emission, optical modulation, saturable absorption, can be harnessed for functions in PICs. With multiple types of 2D materials, the absorption spectrum of the large 2D family can cover an ultrawide optical bandwidth from ultraviolet to microwave holding great promise for optoelectronic applications. Functional devices based on two dimensional (2D) layered transition metal dichalcogenides (TMDs) offer the advantages of low dark current and high speed [1]. In this presentation, we will introduce our recent study for using 2D layered $PtSe_2$ for near-infrared optical photodetectors and modulators. First, we will introduce a high-speed hybrid integrated platinum diselenide on silicon nitride waveguide photodetector. The light is guided in the silicon nitride channel by the design of a bound states in the continuum (BIC) structure for offering a completely planar surface for the hybrid integration [2]. The $PtSe_2$ waveguide photodetector has a responsivity of ~12 mA/W and an optical impulse-response of 35GHz [3]. Secondly, a BIC-waveguide integrated $PtSe_2$ intensity modulator at 1550 nm wavelength with gigahertz response will be described showing the potential of 2D TMD materials for high-speed optoelectronic devices.

References

[1] Yu, Zejie, et al. *"Hybrid 2D-Material Photonics with Bound States in the Continuum"*, Adv. Opt. Mater. (2019)

[2] Wang, Yi, et al. *"High-speed infrared two-dimensional platinum diselenide photodetectors*", Appl. Phys. Lett. (2020)

[3] Wang, Yi, et al. *"Bound-States-in-Continuum Hybrid Integration of 2D Platinum Diselenide on Silicon Nitride for High-Speed Photodetectors",* ACS Photonics (2020)

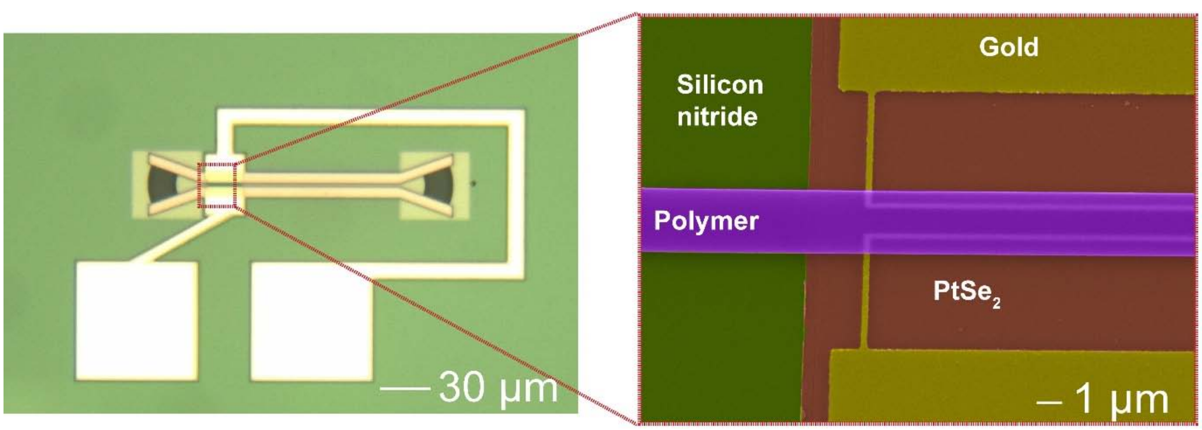

Figure 1. Optical microscope image and False-colour scanning electron microscope (SEM) image of the waveguide-integrated $PtSe_2$ photodetector.

Flexible ultrasensitive phototransistors for biomedical applications

Guodong Zhou and Ni Zhao
Department of Electronic Engineering, The Chinese University of Hong Kong

Near-infrared high-sensitivity photodetectors are the key component to monitor vital health signals noninvasively. Compared to the high-voltage driven avalanche photodiodes and photomultipliers, organic phototransistors based on a bulk heterojunction (BHJ) structure can be self-amplified because of the photoconductive gain mechanism. And they can be tailored to be lightweight, flexible, and work under low voltage. In this presentation, we will introduce our study in flexible ultrasensitive organic phototransistors and their applications for biomedical signal monitoring, including photoplethysmography (PPG) and functional near-infrared spectroscopy (fNIRS). To realize the epidermal/flexible PPG sensor at the fingertip, we explored a new ultrathin encapsulation structure so the sensor can be transferred onto human skin directly. This innovation enables continuous monitoring of heart rate variability and precise tracking of pulse pressure changes at different postures of human subjects. To monitor weak brain signals at the front head, we designed a general tri-layer dielectric approach to achieve stable, low-noise, low-voltage operation phototransistors. Combined with the ultralow noise and portable sampling system, we can monitor brain signals at a maximum distance of three centimeters. These two demonstrations show the organic phototransistors are promising for low operation voltage, low-noise wearable biomedical signal monitoring.

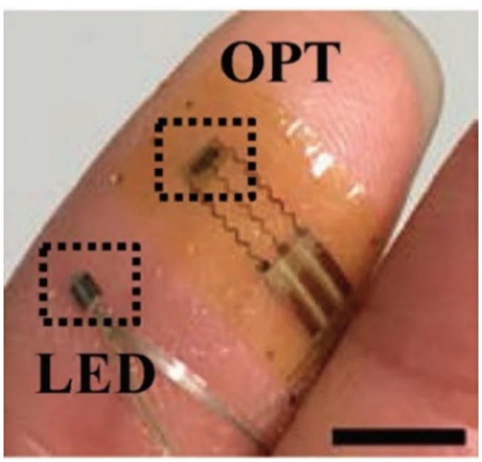

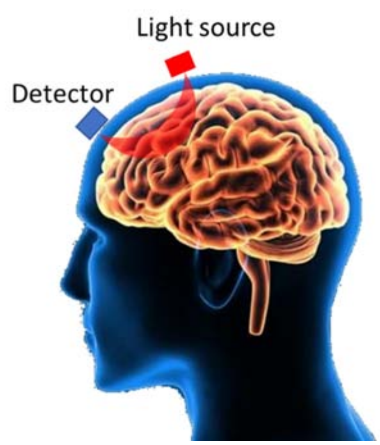

Multi-functional Photonic Processors using Coherent Network of Micro-ring Resonators

Dan Yi, Yi Wang, and Hon Ki Tsang*
Department of Electronic Engineering, The Chinese University of Hong Kong, Hong Kong, Shatin, Hong Kong SAR, P.R. China
**Email: hktsang@ee.cuhk.edu.hk*

Abstract: Silicon photonics have widespread applications in optical communications, photonic sensors, and quantum information processing systems. Different photonic integrated circuits often require similar basic functional elements such as tunable filters, optical switches, wavelength de-multiplexers, optical delay lines, and polarization crosstalk unscrambling. Other optical signal processing functional elements may be needed in specific applications, for example, the differentiation with respect to time of time-varying optical signals, and the implementation of very high extinction interferometers in some integrated quantum photonic circuits. Just as reconfigurable electronic processors in microelectronics have advantages in terms of ready availability and low cost from large-volume generic manufacturing, and are useful for configuration into different functionalities in the form of field-programmable gate arrays (FPGA), here we show how an integrated coherent network of micro-ring resonators can be used in reconfigurable photonic processors. We demonstrate the implementation of optical filters, optical delay lines, optical space switching fabric, high extinction ratio Mach-Zehnder interferometer, and photonic differentiation in a reconfigurable network where the control of the phase in the different arms of the coherent network can determine the implemented functionality. The applications based on the same Reck's architecture (Fig. 1(a)) can be separated into two distinct sets: (i) applications that use the incoherent response of the MRR network (i.e. with basic fabric illustrated as Fig. 1(c)); and (ii) applications that use the coherent response of the network, requiring additional phase shifters as basic fabric illustrated in Fig. 1(b).

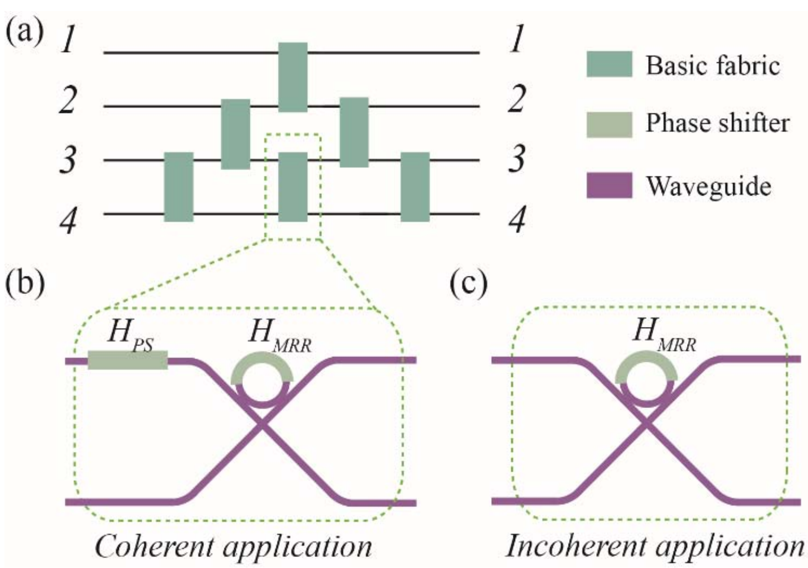

Fig. 1. (a) The topology of architecture. The basic fabric for (b) coherent and (c) incoherent applications.

Water-air optical wireless communication system based on the temporal and spatial properties of waves

Yingjie Shao
Department of Information Engineering, The Chinese University of Hong Kong, Hong Kong SAR, China

Optical wireless communication (OWC) has shown its attractive potential and versatility for various applications for both indoor and outdoor scenarios. For indoor access networks, visible light communication (VLC) utilizing lighting infrastructure has advantages such as no electromagnet interference, license-free, and high security. For outdoor OWC, infrared light has been widely used for free space, such as satellite communication. With the increasing interest in underwater exploration and activities, high-speed underwater wireless data transmission is in high demand. Using blue to green light for underwater wireless communication also attracts more prospects.

We demonstrate a real-time 4K-video transmissions system with low-complexity transmitter-side DSPs over a still water-air optical wireless channel. We also emphasize the time-varying channels and the robust schemes for OWC systems. A bidirectional water-air OWC system through the dynamic water surface waves is experimentally investigated. We then propose to use the precoding scheme to mitigate the wave-induced power fading impairments and experimentally verified the performance improvement. At last, we exploit the spatial and temporal property of waves for the adaptive bit-loading and spatial diversity scheme. The results validate the performance improvement in the throughput and robustness of the water-air OWC system through waves using the proposed scheme.

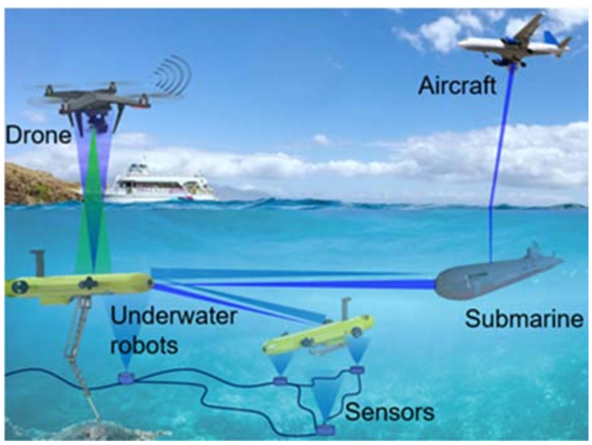

Fig. 1. Illustration of underwater and water-air OWC networks.

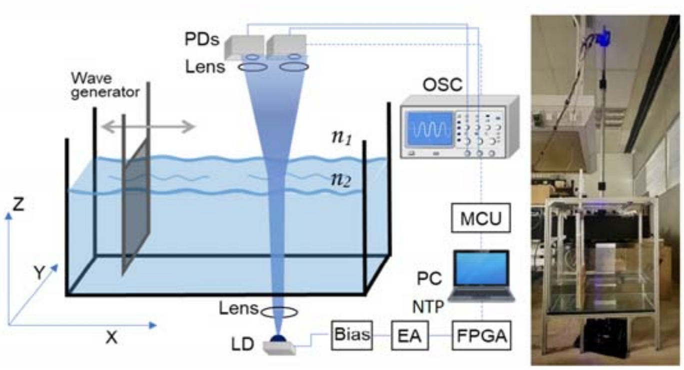

Fig. 2. The experimental setup of the wave-aware water-air OWC system.